MRS Advances © 2019 Materials Research Society
DOI: 10.1557/adv.2019.51

The Voltammetric Hysteresis Behavior and Potential Scan Rate Dependence of a Dye Sensitized Solar Cells

T. M. W. J. Bandara[1*], L. Ajith DeSilva[2], K. Vignarooban[3], S. L. N. Senavirathna[3], R. Luminda Kulasiri[4]

1Department of Physics, University of Peradeniya, Peradeniya, Sri Lanka

[2]Department of Physics, University of West Georgia, Carrollton, GA 30118, USA

[3]Department of Physics, Faculty of Science, University of Jaffna, Jaffna 40000, Sri Lanka

[4]Department of Physics, Kennesaw State University, Marietta Campus, Marietta, GA 30144, USA

[*]corresponding author: awijendr@yahoo.com

ABSTRACT

The voltammetric hysteresis visible in current density versus solar cell potential (J-V) curves is a serious concern because it is known that the performance of Dye-sensitized Solar Cells (DSCs) depends on the direction of the potential and the rate of scan. J-V characteristics of gel electrolyte based DSCs were obtained by varying the scan rate from 0.01 to 0.1 V s^{-1} and the direction from forward bias to reverse bias and reverse bias to forward bias. Three electrolytes were tested, two of them were 100% single salt electrolytes of KI and Hex_4NI, and the other was a mixed salt electrolyte containing KI (75%) and Hex_4NI (25%). DSC containing mixed salts electrolyte exhibited higher efficiency than single salt electrolytes. The energy conversion efficiency with mixed salts increased from 5.9 to 6.4% with the increase of the scan rate from 0.01 to 0.1 V s^{-1}, when the scanning was conducted from forward bias to reverse bias direction. However, when the scanning was carried out with revised polarity a drop of the efficiency was observed with increasing rate of potential scan. Present work emphasizes the importance of reporting the rate and direction of potential scan along with solar cell performance parameters.

1. INTRODUCTION

Solar energy devices are not only reliable renewable energy resources available at low cost but are also zero emission devices without toxic or greenhouse gas effluents. Hence, solar cells are capable of supplying much needed energy for mankind in many useful ways. O'Regan and Grätzel introduced the concept of nano-crystalline TiO_2 thin film-based dye sensitized solar cells (DSC), which are known as Grätzel cells, in 1991. The device uses a metal-organic dye as sensitizer on a nano-crystalline titanium dioxide mesoporous structure [1]. The DSC has been studied intensively for different aspects such as sensitizers and electrolytes [2-4] since then and it has been established as a sustainable alternative to fulfill future energy needs [5].

Generally, in DSCs, the working electrode is a thin layer of mesoporous wide-bandgap semiconductor sensitized by adsorbing dye molecules, which have the ability to capture a wide range of photons from the solar spectrum. The exited electrons in dye are absorbed into the conduction band (CB) of the semiconductor. Metal oxide semiconductors such as TiO_2, ZnO, SnO_2 and ZrO_2 with a variety of morphologies, nano-structures and arrays have been studied as photo-anode materials [3-4]. Amongst them mesoporous TiO_2 has been evolved as the superior material to prepare photo-electrodes with remarkable efficiencies [6]. After electron injection, the ground state of the dye is subsequently restored by electron donation from the reducer (I^-) in the electrolyte. The reducer is regenerated at the counter-electrode where the oxidizer (I_3^-) in the electrolyte obtains electrons from the counter electrode. Many such processes involved in mechanism of solar cells and some give positive influences but others have devastating effect on the cell's performance [7-8]. Time domain of those interactions can be fast and slow processes, for examples electron transition from lowest unoccupied molecular orbitals (LUMO) to the CB of TiO_2 is a fast process with around 0.05-150 ps. However, the electrons from CB of TiO_2 can recombine and fall into the highest occupied molecular orbitals (HOMO) of the dye, which is a slow process with time regime of around 100 ns. Further, LUMO to HOMO transition of the dye is also possible and which is also a slow process with time duration of 20 ns. The slow processes can be influenced by the rate and the direction of the potential scan due to relaxation effects [7-8].

In the present work we study the scan rate dependent on solar cell's parameters of potential used for current-voltage (*I-V*) measurements for quasi-solid DSCs. The scan rate dependence of cell's performance can be understood by studying the capacitive effects at two interfaces, relaxation times of charge transport and transfer. This work emphasizes the importance of reporting the scan rate along with solar cell performance.

2. EXPERIMENT DETAILS

2.1 Electrodes Preparation and Characterization

Two successive layers of TiO_2 were deposited on conducting glass substrate (FTO) in preparing the photo-anode. The first layer was spin coated at 2,300 rpm for 60 s from a slurry which was prepared by grinding 0.5 g of P90 TiO_2 powder (Degassa-Evonik) and 2 ml of HNO_3 (0.1M) for 30 minutes in a mortar. After drying at ambient conditions, it was sintered at 450 °C for 30 minutes. The second layer TiO_2 was applied by Doctor-blade method on top of the first layer. The slurry was prepared in the same way except that 0.1 g of Carbowax and few drops of Triton X 100 (surfactant) were added to the mixture. Then, 2-layer TiO_2 electrode was heated at 450 °C for 30 minutes. Finally, the photo-electrode was completed by sensitizing ruthenium based N719 dye (Solaronix SA).

Model ZEISS EVO LS15 Scanning Electron Microscope (SEM) was used for surface characterization of TiO_2 layers.

2.2 Electrolyte Preparation and Characterization

Chemicals, Polyacrylonitrile (PAN), tetrahexyleammonium iodide (Hex_4NI), iodine, propylene carbonate (PC) and ethylene carbonate (EC) with purity greater than 98% (Sigma Aldrich), were used. For preparing the electrolyte samples, a composition of EC (0.4151 g), PC (0.3851 g), 4TBP (0.0217 g) BMII (0.0126 g) and iodine (I_2) (0.0096 g) kept unchanged while the total weight of KI and Hex_4NI were maintained at 0.0925 g. Appropriately weighed quantities of EC, PC, 4TBP, BMII, KI, and Hex_4NI were mixed in a glass bottle by continuous stirring at room temperature for ~2 h. Then, after adding PAN (0.1 g), the mixture was stirred further for ~30 minutes keeping it at 80 °C until PAN was fully dissolved and the solution became transparent. Finally, the mixture was allowed to cool down to room temperature. Then I_2 was added and stirred over-night to obtain the gel electrolyte. The weight percentages for the mixed-salt electrolyte was, KI (75%) and Hex_4NI (25%) out of the total salt weightage.

The complex impedances of the electrolytes were obtained by sandwiching the samples between two stainless steel electrodes. The complex impedance was measured using an Autolab PGSTAT128N module with Nova software (10 μHz - 32 MHz).

2.3 Assembly of DSC and measurements

The DSC was assembled by sandwiching a thin film of polymer electrolyte between pre-made photo-electrode and a platinum coated glass plate (active area 19 mm^2). It was irradiated by (1.5 AM) 1000 Wm^{-2} using an ABET solar simulator. The *I-V* curves were recorded by using an Autolab PGSTAT128N module with the help of NOVA software. The measurement scanning was done from 0.8 to -0.8 V forward bias direction and revised polarity direction for various scan rates between 0.01-0.1 V s^{-1}.

3. RESULTS AND DISCUSSION

3.1 The structure of TiO_2 films

The SEM mages obtained for the 1st layer (spin coated, P90 size is 14 nm) and 2nd layer (doctor bladed, P25 size is 19 nm) are shown in Figure 1 (a) and (b) respectively. The particle sizes of TiO_2 agree with the images and high surface area due to porous nature of films is visible. This feature is crucial for dye absorption and thus to get better DSC performances.

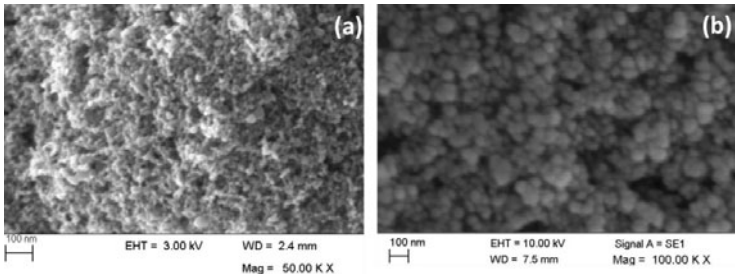

Figure 1. SEM images - (a) spin coated P90 1st layer and - (b) Doctor bladed P25 2nd layer.

3.2 Conductivity in electrolytes

The ionic conductivities in the electrolytes at different temperatures were calculated using Nyquist plots and the results are given in Table 1. The conductivities in all the samples increase with increasing temperature since the mobility and the density of charge carrier are thermally activated. The highest conductivity was obtained for sample *C*. This can be attributed to higher mobility of smaller sized cation K^+ compared to that of Hex^+ The mixed-salt electrolyte exhibited intermediate conductivities as seen from Table1.

Table 1: Ionic conductivities of electrolytes at different temperatures.

Sample	KI/%	Hex_4NI/%	Conductivity /mS cm^{-1}					
			23 /°C	30 /°C	40 /°C	50 /°C	60 /°C	70 /°C
A	0	100	1.70	1.94	2.11	2.23	2.38	2.60
B	75	25	3.53	4.09	4.47	4.98	5.45	5.89
C	100	0	3.74	4.18	4.54	5.19	5.64	6.07

3.3 Solar cell performance

Three DSCs were assembled using electrolyte samples A, B and C. They have energy conversion efficiencies 5.11, 6.38, and 6.00 respectively at the scan rate of 0.1 V s^{-1}. It has been observed that scan rate and polarity dependency on DSC parameters for all three electrolytes. The highest performance was exhibited by the cell containing electrolyte sample B highlighting the mixed cation effect of quasi sold state DSCs. Therefore, electrolyte sample B was selected for further investigation.

3.4 Forward bias to reverse bias (F)

Figure 2 (left) shows the current density against cell potential curves obtained at the different scan rates (0.01-0.1 V s^{-1}) for the DSC prepared with electrolyte sample B. The scanning was conducted from forward bias direction from 0.8 V to -0.8 V. The scan direction is indicated by a solid line arrow. According to the curves, the current density increases with the scan rates. The highest and lowest current densities are observed for 0.1 and 0.01 V s^{-1} scan rates respectively. The change is less significant when the current density reaches near to the open circuit voltage region. For this direction of scan, the measurements are started from a value very close to the V_{oc} thus the performances are less affected by rate of scan. However, it is very significant where at the maximum power densities as seen in Figure 2 (right).

The power density versus cell potential is shown in Figure 2 (right) at different scan rates (0.01-0.1 V s^{-1}) for sample B. The power density values increase with increasing scan rate. The highest value is observed for the scan rate 0.1 V s^{-1}. It is clear that, the power density of this DSC depends on the measurement scan rate.

Calculated DSC parameters, are tabulated in Table 2 labeled columns-F for forward bias. The J_{sc} values increase with increasing scan rate, the highest J_{sc} is 13.63 mA cm^{-1} for 0.1 V s^{-1} scan rate, and the lowest is 13.27 mA cm^{-1} for 0.01 V s^{-1}. Consequently, the highest efficiency is 6.38%, for 0.1 V s^{-1} scan rate, whereas the lowest efficiency is 5.97% for 0.01 V s^{-1}. The dependence of cell parameters on the scan rate is possibly associated with relaxation effects of charge transfer at the two interfaces as well

as mass transport in the electrolyte [7, 8]. As it can be seen, efficiency of the solar cell depends on the scan rate, therefore it is important to report the potential scan rate.

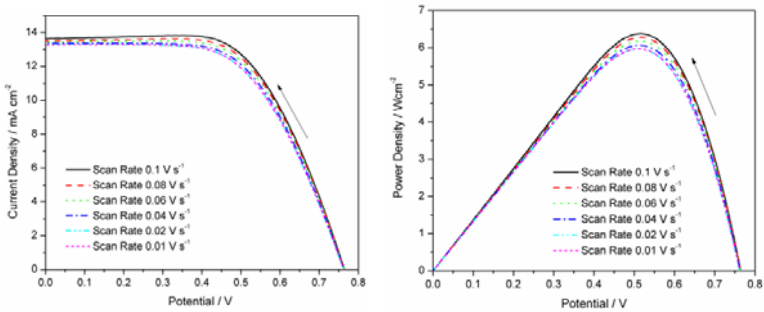

Figure 2. The *J-V* (left) and the power density versus *V* curves (right) at different scan rates between 0.1 - 0.01 V s^{-1}, and the scan direction is from forward (F) bias direction as indicated by the arrows.

Table 2: Cell parameters of DSC under different measurement scan rates between 0.01 V s^{-1} and 0.1 V s^{-1}, for both forward to reverse (columns-F) and reserve to forward (columns-R) bias conditions.

Scan rate / V s^{-1}	J_{sc} / mA cm^{-2}		V_{oc} / mV		*ff* /%		Efficiency (η) / %	
	F	***R***	***F***	***R***	***F***	***R***	***F***	***R***
0.01	13.27	13.42	760.7	758	59.1	57.0	5.97	5.80
0.02	13.30	13.40	761.5	756	59.2	57.1	6.00	5.78
0.04	13.36	13.36	762.5	752	59.5	57.3	6.06	5.76
0.06	13.45	13.32	762.8	748	60.2	57.6	6.18	5.74
0.08	13.52	13.28	764.0	745	60.6	57.6	6.26	5.70
0.10	13.63	13.23	764.6	743	61.2	57.6	6.38	5.66

3.2 Reverse bias to forward bias (R)

Figure 3 (right) shows the *J-V* curves obtained at different scan rates (0.01-0.1 V s^{-1}). For these measurements, the scanning was conducted from reverse bias (-0.8 V) to forward biased (0.8 V) direction as is indicated by an arrow. The power density vs *V* for different scan rates (0.1-0.01 V s^{-1}) is shown in Figure 3 (left). For this scan direction, the power density values increase with decreasing scan rate which is a reversed trend. In this case, the highest power density is for scan rate of 0.01 V s^{-1} and the lowest is for 0.1 V s^{-1}.

The calculated DSC's parameters at different scan rates are given in Table 2 columns-R for scan direction from reverse bias to forward bias. The J_{sc} values decrease from 13.42 to 13.23 mA cm^{-2} with increasing scan rate. The trend of J_{sc}, V_{oc} and η with the change of scan rate shows a completely opposite behavior. The highest V_{oc} and η are 758 mV and 5.80% respectively for scan rate of 0.01 V s^{-1}. Revised trend can be attributed to the effect of reverse biasing and the relaxation behavior of the charge transport [7-8].

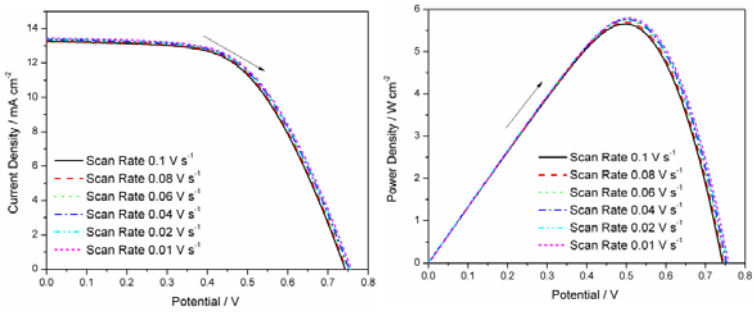

Figure 3. The current density cell potential curves (left) and the power density versus cell potential curves (right) at different scan rates from 0.1 - 0.01 V s^{-1}, scan direction from reverse (R) bias to forward bias direction as indicated by the arrows.

This effect can be further investigated by analyzing capacitances of the cell's interfaces, namely, electrolyte/photo-electrode and electrolyte/counter-electrode interfaces. Based on above discussion, it can be concluded that the potential scan rate is a very important parameter to report. The efficiency of DSC is affected by the scan rate, to determine the nature of measurement artefacts, a further investigation is needed.

4. CONCLUSIONS

The dependence of solar cell parameters on scan rate used for *I-V* measurements has been investigated. *I-V* data was conducted by varying the scan rate from 0.01 to 0.1 V s^{-1} and changing the polarity direction. The J_{sc} increased from 13.27 to 13.63 mA cm^{-2} whereas η increased from 5.97 to 6.38 mA cm^{-2} with increase of scan rate when the scanning is done from forward bias to reverse bias direction. The DSC's η has increased by 6.9 % simply due to increase of scan rate from 0.01 to 0.1 V s^{-1} for forward bias direction. Two different trends of efficiency variation was observed when the scanning direction is altered. The effect will be further investigated by analyzing capacitances of the cell's interfaces. As per results, it can be concluded that the potential scan rate is a very important parameter to report.

REFERENCES

[1] B.O'Regan, M. Grätzel, Nature, **353,** 737-740 (1991).
[2] M.K. Nazeeruddin, F. De Angelis, S. Fantacci, A. Selloni, G. Viscardi, P. Liska, S. Ito, B. Takeru, M. Grätzel, Journal of the American Chemical Society, **127**, 16835-16847 (2005).
[3] A.F. Nogueira, C. Longo, M.A. De Paoli, Chemistry Reviews, **248,** 1455-1468 (2005).
[5] Khan MZ, Al-Mamun MR, Halder PK, Aziz MA. Renew. Sust. Energ. Rev. **71,** 602-17 (2017).
[4] M.K. Nazeeruddin, E. Baranoff, M. Gratzel, Sol. Energy, **85**, 1172–1178 (2011).
[6] A. Jena, S.P. Mohanty, P. Kumar, J. Naduvath, V. Gondane, P. Lekha, J. Das, H.K. Narula, S. Mallick, P. Bhargava, Transactions of the Indian Ceramic Society, **71,** 1-16 (2012).

[7] J. Gong, J. Liang, K. Sumathy, Renew. Sust. Energ. Rev., **16,** 5848-5860 (2012).
[8] G. Boschloo, A. Hagfeldt, Accounts of Chemical Research, **42,** 1819-1826 (2009).